

microRNA Expression Pattern Modulates Temozolomide Response in GBM Tumors with Cancer Stem Cells

Gulcin Tezcan · Berrin Tunca · Ahmet Bekar · Matthias Preusser ·
Anna Sophie Berghoff · Unal Egeli · Gulsah Cecener · Gerda Ricken ·
Ferah Budak · Mevlut Ozgur Taskapilioglu · Hasan Kocaeli · Sahsine Tolunay

Received: 2 January 2014 / Accepted: 13 March 2014 / Published online: 2 April 2014
© Springer Science+Business Media New York 2014

Abstract Temozolomide (TMZ) is widely used to treat glioblastoma multiforme (GBM). Although the *MGMT* gene methylation status is postulated to correlate with TMZ response, some patients with a methylated *MGMT* gene still do not benefit from TMZ therapy. Cancer stem cells (CSCs) may be one of the causes of therapeutic resistance, but the molecular mechanism underlying this resistance is unclear. microRNA (miRNA) deregulation has been recognized as another chemoresistance modulating mechanism. Thus, we aimed to evaluate the miRNA expression patterns associated with chemoresistance that is dependent on the CSC status in GBM tumors to identify therapeutic

biomarkers. CSCs were identified in 5 of 20 patients' tumor tissues using magnetic separation. CSC (+) tumors displayed a significant induction of CpG island methylation in the *MGMT* gene promoter ($p = 0.009$). Using real-time reverse transcription polymerase chain reaction (qRT-PCR), 9 miRNAs related to GBM (mir-181b, miR-153, miR-137, miR-145, miR-10a, miR-10b, let-7d, miR-9, and miR-455-3p), which are associated with cell cycle and invasion was analyzed in tumor samples. Low miR-181b and high miR-455-3p expression levels were detected ($p = 0.053$, $p = 0.004$; respectively) in CSC (+) tumors. Analysis revealed a significant correlation between miR-455-3p expression and Smad2 protein levels as analyzed by immunohistochemistry in CSC (+) tumors ($p = 0.002$). Thus, miR-455-3p may be involved in TMZ resistance in *MGMT* methylated CSC (+) GBM patients. Further studies and evaluations are required, but this miRNA may provide novel therapeutic molecular targets for GBM treatment and new directions for the development of anticancer drugs.

G. Tezcan · B. Tunca (✉) · U. Egeli · G. Cecener
Department of Medical Biology, Medical Faculty, Uludag
University, Bursa, Turkey
e-mail: btunca@uludag.edu.tr

A. Bekar · M. O. Taskapilioglu · H. Kocaeli
Department of Neurosurgery, Medical Faculty, Uludag
University, Bursa, Turkey

M. Preusser · A. S. Berghoff
Division of Oncology, Department of Medicine I,
Comprehensive Cancer Center Vienna, Medical University of
Vienna, Vienna, Austria

G. Ricken
Institute of Neurology, Comprehensive Cancer Center Vienna,
Medical University of Vienna, Vienna, Austria

F. Budak
Department of Microbiology, Medical Faculty, Uludag
University, Bursa, Turkey

S. Tolunay
Department of Pathology, Medical Faculty, Uludag University,
Bursa, Turkey

Keywords Glioblastoma · Cancer stem cell ·
Temozolomide · microRNA · Therapy

Introduction

Glioblastoma multiforme (GBM) is the most common type of primary malignant brain tumors and associated with an aggressive clinical course (Louis et al. 2007). Despite aggressive multimodal therapies, such as surgical resection, chemo- and radio-therapy, only a small subgroup of GBM patients survive longer than 5 years (Stupp et al. 2009). The median overall survival time remains approximately 14.6 months, and the 5-year survival rate is only 9.8 % (Reya et al. 2001).

Recent studies have demonstrated that malignant tumors may contain a stem-like cell population, namely cancer stem cells (CSCs), which is responsible for the maintenance and propagation of these tumors (Reya et al. 2001). Research investigating the CSC hypothesis may provide insights into therapeutic resistance and tumor recurrence, and underscore the complexity of cancer (Lathia et al. 2011). There is increasing evidence that GBM might contain and arise from CSCs (Ignatova et al. 2002; Singh et al. 2003). CSCs in GBM tumors demonstrate different characteristics compared to other GBM cells. There are several lines of evidence suggesting that brain tumors arise from the proliferation of aberrant neural stem cells (Oliver and Wechsler-Reya 2004). For example, many brain tumors contain neuronal and glial elements and express CD133 and the intermediate filament Nestin (Rorke 1997; Nakano and Kornblum 2006). In addition, research has shown that these cells express many gene characteristics of neural stem cells, including *CD44*, *Octamer-binding transcription factor 4 (OCT-4)*, *Integrin (ITGA1)*, and *Vimentin (VIM)*, with reverse transcriptase polymerase chain reaction (qRT-PCR) analysis (Dirks 2005; Cheng et al. 2012). Studies have also demonstrated that CSCs can proliferate in the presence of epidermal growth factor (EGF), basic fibroblast growth factor (bFGF), leukemia inhibitory factor (LIF), and B27 in serum free medium (Nakano and Kornblum 2006; Hemmati et al. 2003).

CSCs are considered as the most chemoresistant cell fraction in GBM and are believed to be responsible for relapse (Altaner 2008; Sanchez-Martin 2008; Persano et al. 2012). Studies have demonstrated that temozolomide (TMZ) is mainly ineffective against CSCs, which are characterized by high methylated *O-6-methylguanine-DNA methyltransferase (MGMT)* expression (Persano et al. 2012; Liu et al. 2006; Pistollato et al. 2010). Patients with *MGMT* methylation who are treated with TMZ show an overall survival time increase from 15.3 to 23.4 months. Conversely, a group of patients with unmethylated *MGMT* received no significant benefit from treatment with TMZ (11.8 vs. 12.6 months) (Nakano and Kornblum 2006; Hemmati et al. 2003). However, the favorable outcomes for these patients cannot be linked solely to their *MGMT* methylation status. Chemotherapy resistance may also be modulated by microRNA (miRNA) regulation. miRNAs are small, non-coding RNAs (18–25 nucleotides in length) that bind to complementary 3'UTR regions of target mRNAs, regulating transcription of the target gene (Bartel 2009; Calin and Croce 2006). It is predicted that miRNAs regulate the expression of up to 70 % of human genes and potentially play a role in the regulation of nearly every genetic pathway including chemoresistance (Lewis et al. 2005; Esquela-Kerscher and Slack 2006; Kreth et al. 2013). For this reason, understanding the regulatory role of

miRNAs in CSC (+) GBM tumors may clarify the molecular mechanisms associated with chemoresistance in these patients.

In this study, we isolated CSC-enriched primary GBM tumors using magnetic separation and examined the association of *MGMT* methylation status and different expression patterns of 9 miRNAs related with cell-cycle regulation and the invasion status between CSCs (+) and CSCs (–) tumors to determine potential therapeutic biomarkers for identifying personal drug resistance status and new therapy approaches.

Materials and Methods

Patient Selection

A total of 20 GBM patients (11 male and 9 female) with an age range of 48–73 years (mean age \pm SEM, 60.95 ± 1.77 years) were selected as the sample cohort, and the control tissues samples taken from 5 epilepsy patients were used as a control group to evaluate the regulation of CSC markers. Informed consent was obtained from all patients. The study was approved by the local Ethics Committee (2011-17/07) and conformed to the ethical standards of the Helsinki Declaration.

Tumor Specimens

GBM tissues and control, and non-tumoral epileptic tissues were obtained from patients during surgery and were assessed by a pathologist in the operating room at Uludag University Medical Faculty. Independent pathologists classified the tumors by type and grade in accordance with the WHO histological classification of central nervous system tumors.

IDH Mutation Analyses

IDH1(R132H) protein expression was determined immunohistochemically by examining formalin-fixed and paraffin-embedded (FFPE) blocks of resected tumor tissue. Tissue blocks were cut at a thickness of 3–4 μ . Sections underwent heat-induced antigen retrieval for 60 min and were incubated with the monoclonal IDH1(R132H) antibody (clone DIA-H09; Dianova, Hamburg, Germany) at a dilution of 1:30 for 60 min. The antibody specifically recognizes the IDH1-R132 H mutation status. Detection of immunolabeling was performed using the Flex + Mouse system (Dako, Glostrup, Denmark) with diaminobenzidine as a chromogen. The presence or absence of tumor cell immunolabeling was evaluated by three observers. The expression of IDH1(R132H) was determined using a

2-tiered semiquantitative scoring system. Cases with cytoplasmic/nuclear expression of the mutant IDH1(R132H) protein in tumor cells were scored as positive. The absence of immunostaining was scored as negative. No case with partially positive or partially negative staining of tumor cells was encountered.

MGMT Methylation Analyses

Genomic DNA was extracted from cell cultures with and without CSCs using QIAamp DNA mini kits (Qiagen, Germantown, MD). All DNA samples were assessed for DNA quantity and quality using the NanoDrop 2000 Spectrophotometer. Protein and chemical contamination was determined by obtaining the 260:280 ratios for each DNA sample. DNA samples with 1.8–2.0 for the 260:280 ratios were selected for the *MGMT* methylation analyses. An EpiTech Methyl quantitative PCR assay (Qiagen, Germantown, MD) was used to analyze the *MGMT* gene promoter methylation levels. Briefly, DNA was selectively digested by methylation-sensitive enzymes (cut unmethylated and partially methylated DNA, leaving only hypomethylated DNA) and methylation-dependent restriction enzymes (cut any methylated DNA, leaving only unmethylated DNA) according to the manufacturer's protocol. After digestion, DNA was quantified using qRT-PCR. The relative concentrations of differentially methylated DNA were determined by comparing the amount of each digest with that of mock digest (no enzyme added), using the software provided by the manufacturer (Qiagen, Germantown, MD). Using EpiTech Methyl quantitative PCR assay, *MGMT* methylation analyses were triplicated for each sample. In addition, to verify the reliability of our data, promoter methylation status of each cases were also analyzed with methylation specific PCR as described previously (Cecener et al. 2012).

Primary Cell Culture and Cell Sorting

Glioma tissues were processed under sterile conditions in a laminar flow hood. Tumors were washed with sterile PBS with 5 % antibiotic/antimycotic solution (Paa, Cölbe, Germany) and subjected to enzymatic dissociation. Tumor cells were then resuspended and grown in Dulbecco's Modified Eagle's Medium-F12 (DMEM-F12; Lonza, Verriers, Belgium) containing L-glutamine (Lonza) supplemented with 10 % fetal bovine serum (FBS, Lonza), 1 mM sodium pyruvate (Lonza), and 1 % Antibiotic/Antimycotic solution (Paa), incubated in a 5 % CO₂ humidified incubator at 37 °C. The cultured cells were maintained for 7 days. The medium was then replaced with serum-free growth medium consisting of DMEM F-12 medium (1:1) supplemented with heparin (5 µg/ml, Fisher Scientific

Company L.L.C., Pittsburgh, PA), human recombinant EGF (50 ng/ml; Biological Industries, Kibbutz Beit-Haemek, Israel), bFGF (20 ng/ml; Biological Industries), B27 (2 %, Gibco-BRL, Gaithersburg, MD), LIF (10 ng/ml; Millipore, Darmstadt, Germany), and Antibiotic/Antimycotic solution (1 %, Paa). Magnetic separation of CSCs was performed using the Miltenyi Biotec CD133 Cell Isolation kit (Miltenyi Biotec GmbH, Germany). CD133+sorted cell populations were resuspended in stem cell medium.

Validation of Cancer Stem Cell Markers

Flow Cytometry

After CD133+cell sorting and proliferation in stem cell medium, 1X10⁶ cells were washed twice with Ca²⁺ and Mg²⁺-free PBS (Lonza), trypsinized (0.025 % trypsin/EDTA) (Gibco), and harvested in Ca²⁺ and Mg²⁺-free PBS.

Tumor cells were collected and stained with 10 µl anti-CD133 antibody (CD133/2 (293C3)-PE Human monoclonal IgG1; 1:10; Miltenyi Biotec) or Mouse IgG2b-PE isotype control antibody (Miltenyi Biotec). After incubation for 30 min, cells were washed in Cell WASH (BD, Erembedegem, Belgium), and CD133 staining was analyzed using a flow cytometry FACSCanto (Becton–Dickinson, USA).

For detection of the Nestin expression levels, cells were fixed with Permeabilizing Solution 2 (BD, USA) for 10 min at room temperature, washed twice with Cell WASH (BD), and stained with 10 µl anti-Nestin antibody (Alexa flour 647 mouse anti-Nestin; BD) or mouse (MOPC-21) IgG1 isotype control (Alexa (R) 488) mouse mAb (BD). After incubation for 30 min, cells were washed in Cell WASH (BD), and Nestin staining was analyzed using a flow cytometry FACSCanto (Becton–Dickinson, USA).

RNA Extraction and RT–PCR Assay

After flow cytometric analyses, cell populations containing CD133 and Nestin (+) cells and the tissue samples of the control group were subjected to total RNA extraction using RNeasy kits (Qiagen, Germantown, MD) and were then reverse transcribed using Transcriptor High Fidelity cDNA Synthesis Kits (Roche Diagnostics, Mannheim, Germany). The samples were then analyzed using RT-qPCR to profile the *ITGA* (NM_181501), *VIM* (NM_003380), *CD44* (NM_000610), and *OCT4* (NM_002701) expression levels; we also evaluated the expression level of the human *Actin Beta* (*ACTB*) housekeeping gene. Gene expression analyses were duplicated for each sample. Only samples with C_t

values less than 35 were included in further analyses. PCR was carried out in a 20 ml reaction mixture that contained 5 μ l cDNA as a template, 10 μ M specific oligonucleotide primer pairs, and SYBR Green qPCR master Mix (Qiagen, Germantown, MD). The cycle parameters were as follows: 95 °C for 10 min, 45 cycles at 95 °C for 15 s, and 60 °C for 60 s, followed by melting curve analyses in the LightCycler 480II (Roche Diagnostics, USA). Genomic DNA contamination was analyzed by performing a no reverse transcription control with RNA samples using an *ACTB* RT-qPCR primer assay. The initial copy number in the samples and threshold cycle (C_t) for mRNA expression was determined using the Light Cycler 480II software (Roche Diagnostics, Indianapolis, USA). The $2^{-\Delta C_t}$ method was used to calculate the fold change in mRNA expression between the tested samples (Livak and Schmittgen 2001).

miRNA Expression Analysis

Total RNA (5 ng) of cells with and without CSCs was reverse transcribed using the RT2 miRNA First Strand Kit (Qiagen, Germantown, Maryland, USA). The samples were analyzed for the presence and differential expression of 9 miRNAs related to drug resistance and GBM development using RT2 miRNA primer assays (RT2 Profiler; Qiagen, Frederick Md, USA) according to the manufacturer's instructions. The accession numbers of the primers are shown in Table 1. miRNA expression analyses were duplicated for each sample. Thermal cycling conditions for all assays were 95 °C for 10 min, 45 cycles at 95 °C for 15 s, and 60 °C for 30 s, followed by melting curve analysis in the LightCycler 480II (Roche Diagnostics, Indianapolis, USA). RNA input was normalized to endogenous control SNORD 48 for miRNAs and the TATA-binding protein for protein encoding genes. The initial copy number in the samples and the threshold cycle (C_t) for miRNA expression were determined using the Light Cycler 480II software (Roche Diagnostics, Indianapolis, USA). The miRNA Reverse Transcription Control Assay was used to test the efficiency of

the miScript II Reverse Transcription Kit reaction using a primer set to detect a template synthesized from the kit's built-in miRNA External RNA Control. Positive PCR control assays were used to test the efficiency of the polymerase chain reaction chemistry and of the instrument using a pre-dispensed artificial DNA sequence and a primer set designed to detect the sequence. The $2^{-\Delta C_t}$ method was used to calculate the fold change in miRNA expression between the tested samples (Livak and Schmittgen 2001).

miRNA Target Prediction

miRNA target genes were identified using the miRWalk online database (<http://www.umm.uni-heidelberg.de/apps/zmf/mirwalk>). miRWalk provides information on published pathway targets from the KEGG (<http://www.genome.jp/kegg>) and BioCarta (<http://www.biocarta.com/>) pathway databases. The gene functions were obtained from KEGG and NCBI-Gene (<http://www.ncbi.nlm.nih.gov>).

Immunohistochemistry of Target Proteins

FFPE tumor tissues were cut at a thickness of 3–4 μ . Sections underwent heat-induced antigen retrieval in 10 mM citrate buffer (pH 6) for Smad 2 staining and Tris/EDTA pH 9 buffer (target retrieval solution high pH; Dako, Glostrup, Denmark) for Bcl2 staining. Immunohistochemical stainings were performed manually. Monoclonal mouse anti-human Smad2 antibody (Santa Cruz Biotechnology, Santa Cruz, CA) was diluted at 1:200 and incubated overnight. Mouse monoclonal anti-human Bcl2 antibody (Dako, Glostrup, Denmark) was diluted at 1:50 and incubated overnight. Detection of immunolabeling was performed using the Dako REAL™ EnVision™ Detection System (Dako, Glostrup, Denmark) according to the manufacturers' instructions, with diaminobenzidine as a chromogen. The sections were then counterstained with hemalaun, dehydrated, cleared in xylene, and mounted. For both Bcl2 and Smad2 stainings, colon carcinoma samples with known immunoexpression levels were used as positive controls. The presence or absence of tumor cell immunolabeling was evaluated by three observers. Tumor cell immunolabeling was evaluated independently from the results of other analyses and clinical data. According to the previous publications, Bcl2 was evaluated semi-quantitatively for the presence of greater than or less than 10 % of cells showing specific perinuclear, cytoplasmic staining (Revelos et al. 2005). The immunohistochemical staining of Smad2 was evaluated separately for the cytoplasm and the nucleus according to previous publications (Kloth et al. 2008). Because no variety in staining intensity was observed for the nuclear immunohistochemical signal of

Table 1 Accession numbers of the miRNA primers

miRNA Sanger ID	miRNA accession number
mir-181b	MIMAT0000257
miR-153	MIMAT0000439
miR-137	MIMAT0000429
miR-145	MIMAT0000437
miR-10a	MIMAT0000253
miR-10b	MIMAT0000254
let-7d	MIMAT0000065
miR-9	MIMAT0000441
miR-455-3p	MIMAT0004784

Smad2, the percentage of labeled nuclei is given. Cytoplasmatic staining was evaluated based on intensity (weak, moderate, or strong).

Statistical Analysis

To study the potential influence of clinical features, a statistical analysis was carried out. The Chi-squared (χ^2) test, Fisher's exact test, and RT² Profiler PCR Array Data Analysis (<http://www.sabiosciences.com/pcr/arrayanalysis.php>) were used to compare the results of the PCR array analysis with characteristics of CSC (+) and CSC (–) cases. Independent T-tests were used to evaluate the *MGMT* methylation rates, Pearson correlation analyses were performed to analyze the correlations between miRNA expressions and target protein levels, and median survival curves were plotted using the Kaplan–Meier method with SPSS 16 statistical software. The log-rank test was used to assess survival differences between the groups. The overall survival was defined as the intermediate time interval between sampling and final follow-up. Confidence intervals of 95 % were calculated using the associated estimated standard errors. A *p* value < 0.05 was considered statistically significant.

Results

Clinical Data

Twenty patients diagnosed with GBM entered this study. The 11 men and 9 women were aged 48–73 years, and the median age at the time of diagnosis was 62.5 ± 1.76 years. Two patients were 50 years of age or older at the time of diagnosis. Primary tumors were localized in the brain's parietal region in 4 cases, the frontal region in 9 cases, the temporal region in three cases, the thalamic region in 2 cases, and the occipital region in 1 case. The most common symptoms at diagnosis were severe headache and seizure [7 (33.3 %) and 5 (23.8 %) cases, respectively]. Speech difficulties and weakness were observed in 4 (19 %) patients, personality changes and mood and character alterations were observed in 2 (9.5 %) patients, and 16 patients (76.1 %) suffered neurological deficits; no patients had neurological deficits other than paresis.

IDH1 Mutation Analysis

IDH1 mutations have been described with a high prevalence of 60–80 % in diffuse gliomas, anaplastic astrocytomas, secondary GBM, and oligodendrogliomas of WHO grade II and WHO grade III, but with a low occurrence of 5–15 % in primary GBM in previous studies (Ichimura et al. 2009; Nobusawa et al. 2009; Leibetseder et al. 2013).

In the current study, all tumors were negative for the IDH1(R132H) mutation. Thus, all of the tumors in this study were identified as primary GBM.

Selection of Tumor Lines Containing CSCs

CD133 has been identified as a marker of CSCs in recent studies (Okamoto et al. 2007; Galli et al. 2004; Brescia et al. 2013). After screening the primary cultured cells of 20 GBM patients, 5 formed separate colonies in 10 % FBS/DMEM/F-12 culture medium for 3–6 passages (Fig. 1), which transformed into floating neurospheres when placed in CSC medium (Fig. 1). Magnetic separation was used to separate CD133 (+) cells from these five primary cultured cell lines; isolated cells were grown in CSC medium for two passages until there was a sufficient number of cells for further analysis.

To avoid ignoring the differentiation potential of CSCs after 2 passages, we used flow cytometry to analyze the expression levels of CD133 and Nestin (well-known stem cell markers) (Rorke 1997; Nakano and Kornblum 2006) in the five primary cultured cell lines. The detected CD133 expression levels were 1.5, 12.9, 4.5, 6, and 4.4 % in the cases numbered P3, P4, P8, P9, and P12, respectively (Fig. 2). The detected Nestin expression levels were 36.5, 3.1, 32.4, 2.3, and 25.7 % in the cases numbered P3, P4, P8, P9, and P12, respectively (Fig. 2).

The expression levels of *ITGA*, *VIM*, *CD44*, and *OCT4*, which are related to cell “stemness,” were also analyzed in both CSC (+) and CSC (–) tumor cell lines using real-time PCR. These genes were upregulated at least twofold in CSC (+) primary tumor cells compared to the average $2^{-\Delta C_t}$ value of the control samples (Table 2).

Depending on the CSC status of tumors, basic clinical and tumor characteristics such as the age at diagnosis, gender, localization, and the glial fibrillary acidic protein (GFAP), p53 and Ki-67 proliferation index of patients were analyzed using the χ^2 and Fisher exact tests. The relationship between the clinical profiles and pathological features of patients and the CSC status of tumors are summarized in Table 3. CSC (+) cases were significantly younger than CSC (–) cases ($p < 0.001$). Additionally, in CSC (+) tumors, the GFAP and Ki-67 staining intensities were significantly stronger ($p < 0.001$, $p = 0.007$; respectively). However, there were no significant associations between the patient gender, tumor localization, p53 staining status, and CSC positivity.

miRNA Expression Profiles of GBM Cells with CSCs

The expression levels of mir-181b, miR-153, miR-137, miR-145, miR-10a, miR-10b, let-7d, miR-9, and miR-455-

Fig. 1 CSC (+) GBM cell proliferation in culture conditions; **a** 2nd day of culture, **b** 7th day of culture, **c** 1st day of culture after CD133 (+) cell separation, **d** early phase neurosphere formation of CSCs ($\times 40$)

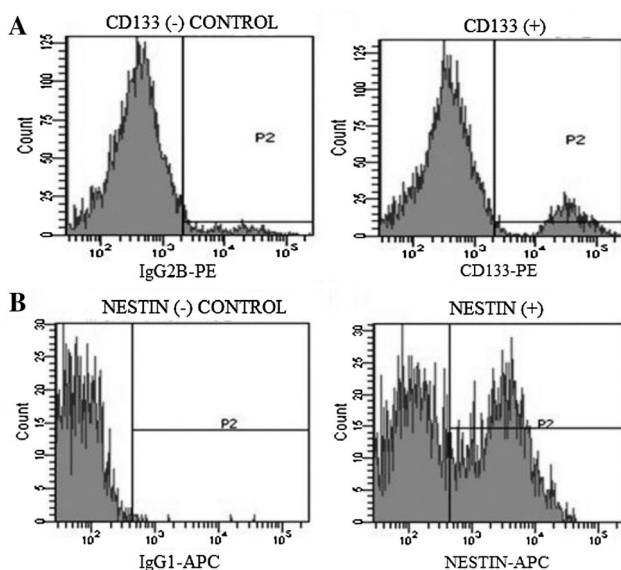
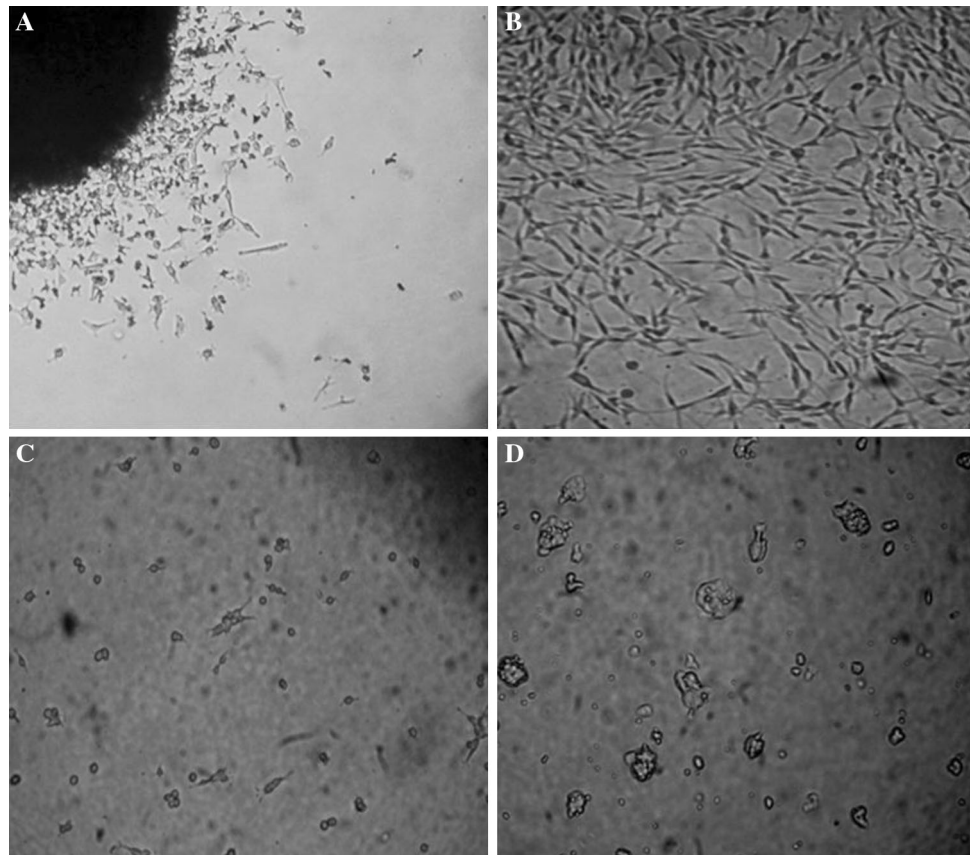


Fig. 2 Flow cytometric images. **a** CD133 and **b** Nestin status of the CSCs

3p were evaluated in all samples and the fold changes were compared between CSC (+) and CSC (-) tumors. The miR-455-3p expression levels were significantly higher in the CSC (+) cases ($p < 0.01$). In addition, miR-181b, miR-

153, miR-137, miR-145, let-7d, and miR-9 were down-regulated in CSC (+) patients. Although miR-181b regulation was almost significant, the differences calculated for miR-153, miR-137, miR-145, let-7d, and miR-9 were not statistically significant ($p > 0.05$, Table 4).

MGMT Methylation Analysis

GBM tumors that contain CSCs displayed a significant induction of CpG island methylation in the *MGMT* gene promoter compared to tumors without CSCs [the mean methylation rates of tumors with and without CSCs were $50 \% \pm 0.00$ and $26.5 \% \pm 6.85$, respectively, calculating using an independent sample *T*-test; $p = 0.009$, (95 % CI 5.9, 35.3)]. However, according to Pearson correlation analyses, there were no significant correlations between the *MGMT* status and miR-181b or miR-455-3p expression levels ($r = -0.064$, $p = 0.788$; $r = 0.161$, $p = 0.498$, respectively).

Identification of Differentially Expressed miRNA Target Genes Using Bioinformatic Analysis

The target genes of the significantly altered miRNAs miR-181b and miR-455-3p were identified using the miRWalk online database and the KEGG and BioCarta pathway

Table 2 mRNA expression levels of CSCs markers in CD133 positive GBM cells

	P3		P4		P8		P9		P12		Control*
	2 ^{-ΔC_t}	Fold change	Average (2 ^{-ΔC_t})								
ITGA	1.9453	8894.3081	0.0021	9.8401	0.0020	58.8376	0.162668	743.7462	0.2058	941.4017	0.0002
VIM	6.2333	9598.9885	0.5586	860.2825	0.5580	81.4965	2.411616	3713.7646	0.0421	64.8335	0.0006
CD44	0.7845	1434.8326	0.2517	460.3753	0.2510	43.9158	0.283221	517.9492	0.1158	211.8158	0.0005
OCT4	3.7580	660.1576	0.0028	0.4900	0.0020	2.0000	0.325335	57.1494	0.4673	83.6716	0.0056

P Patient’s tumor tissue

* Epileptic tissue samples were used as non-tumoral control samples

Table 3 The association of the biopathological features of patients and the CSC status

Characteristics	CSCs (+) (%)	CSCs (-) (%)	p value
Median age at diagnosis (year)			<0.001**
<50	2 (10)	0 (0)	
>50	3 (15)	15 (75)	
Gender			0.655**
Male	1 (5)	10 (50)	
Female	4 (20)	5 (25)	
Tumor localization			0.075*
Parietal	2 (10)	2 (10)	
Frontal	2 (10)	7 (35)	
Temporal	0 (0)	3 (15)	
Thalamic	1 (5)	1 (5)	
Occipital	0 (0)	2 (10)	
GFAP			<0.001**
+	5 (25)	14 (70)	
-	0 (0)	1 (5)	
p53			0.371**
>50 %	4 (20)	8 (40)	
<50 %	1 (5)	7 (35)	
Ki-67 (%)			0.007**
≤499	1 (5)	3 (35)	
≥500	4 (20)	12 (60)	

* Evaluated using the χ^2 test using SPSS 16.00 software for Windows (IBM, Chicago, IL)

** Evaluated using the Fisher exact test using SPSS 16.00 software for Windows (IBM, Chicago, IL)

databases. The predicted target genes were validated by searching recent literature. The function of these genes was defined according to NCBI-Gene database. The validated genes for miR-181b and miR-455-3p are involved in signaling pathways related to cellular processes that include apoptotic regulation (Table 5).

miR-181b targets at least *ATM*, *BCL2*, *Transforming growth factor beta (TGF- β)*, *TIMP3*, and *MCL-1*, while miR-455-3p targets *SMAD2*, *ACVR2B*, *LTBR*, and *EI24*, which

are implicated in cancer formation. According to the miR-Wak databases, *BCL2* is a pro-apoptotic gene that is also a predicted target of miR-153, miR-137, miR-145, miR-10a, miR-10b, let-7 d, and miR-9. In addition, *SMAD2* is one of the well-known *TGF- β* dependent anti-apoptotic genes. Aberrant expression of *SMAD2* has been reported in several GBM studies (Zhang et al. 2006). We, therefore, evaluated the protein products of the *BCL2* and *SMAD2* genes using immunohistochemical analyses to validate the effects of miR-181b and miR-455-3p in our study cohort. The images from the Bcl2 and Smad2 stainings are shown in Fig. 3.

According to Pearson correlation analyses, nuclear Bcl2 staining revealed negative correlations with miR-181b, miR-153, miR-137, miR-145, miR-10a, miR-10b, let-7d, and miR-9, but not at significant levels. However, there was a significant relationship between miR-455-3p expression and cytoplasmic Smad2 staining of the samples (Table 6).

Correlation Between CSC Presence and Survival

Kaplan–Meier plots comparing the median survival rates of patients with CSC (+) and CSC (-) tumors are presented in Fig. 4. The median follow-up time was 10 ± 1.28 months (range 1–23 months). The median survival was shorter in the CSC (+) cases than in the CSC (-) cases, but the difference was not significant (log-rank $p = 0.610$; Fig. 4).

Correlation Between miR-181b and miR-455-3p Expression and Survival

The median survival time was longer for patients with high miR-181b expression and low SMAD2 expression. However, the differences were not statistically significant (log-rank $p = 0.610$, $p = 0.097$, respectively, Fig. 5).

Discussion

In the present study, primary GBM tissue samples, identified clinically, pathologically, and by IDH1-R132H

Table 4 miRNA expression status of CSC (+) GBM tumors

miRNA	CSCs (–) $2^{(-\text{Avg.}(\Delta\text{ct}))}$	CSCs (+)	Fold change	Fold regulation	<i>p</i> value*	95 % CI
mir-181b	4.11435	0.02243	0.0055	Down	0.05325	(0.00001, 0.02)
miR-153	0.00112	0.00037	0.3376	Down	0.67240	(0.00001, 1.01)
miR-137	0.00129	0.00051	0.4000	Down	0.35472	(0.00001, 1.19)
miR-145	0.00666	0.00021	0.0325	Down	0.12048	(0.00001, 0.10)
miR-10a	0.00108	0.00063	0.5894	Down	0.11444	(0.00001, 1.94)
miR-10b	0.00131	0.00067	0.5105	Down	0.15694	(0.00001, 1.72)
let-7d	0.07988	0.00019	0.0024	Down	0.10925	(0.00001, 0.01)
miR-9	0.03782	0.00022	0.0059	Down	0.26610	(0.00001, 0.02)
miR-455-3p	0.00221	0.11858	53.643	Up	0.00476	(0.00001, 166.83)

* Evaluated with the independent sample *T*-test using RT2 profiler PCR array data analysis

Table 5 Predicted targets of miR-181b and miR-455-3p

miRNA	Gene symbol ^{a,b}	Gene description ^c	References
miR-181b	<i>ATM</i>	Ataxia telangiectasia mutated	Bisso et al. (2013)
	<i>BCL2</i>	B-cell CLL/lymphoma 2	Zhu et al. (2010), Calin et al. (2007)
	<i>TGF-β</i>	Transforming growth factor, beta 1	(Wang et al. 2012, 2010)
	<i>TIMP3</i>	Tissue inhibitor of metalloproteinase 3	Wang et al. (2010)
	<i>MCL-1</i>	Myeloid cell leukemia sequence 1	Zhu et al. (2012), Visone et al. (2011)
miR-455-3p	<i>SMAD2</i>	SMAD family member 2	Swingler et al. (2012), Ujifuku et al. (2010)
	<i>ACVR2B</i>	Activin A receptor, type IIB	Swingler et al. (2012), Ujifuku et al. (2010)
	<i>LTBR</i>	Lymphotoxin beta receptor (TNFR superfamily, member 3)	Ujifuku et al. (2010)
	<i>E124</i>	Etoposide induced 2.4 mRNA	Ujifuku et al. (2010)

^a From the KEGG and BioCarta pathway databases

^b From the miRWalk database

^c From the NCBI-Gene database

immunostaining, from 20 patients were analyzed for their stemness properties; 5 of the tumors were classified as CSC (+). Patients with CSC (+) tumors were significantly younger ($p < 0.001$), and the GFAP and Ki-67 staining intensities were stronger in CSC (+) tumors ($p < 0.001$, $p = 0.007$; respectively). One of the characteristic features of CSCs is their resistance to chemotherapy and radiation therapy (Reya et al. 2001). To the best of our knowledge, the hypermethylation status of *MGMT* is an important predictor of response to TMZ-based chemotherapy in patients with GBM (Hegi et al. 2005; Weller et al. 2013). Therefore, in this study, the *MGMT* promoter methylation status of CSC (+) and CSC (–) tumors was evaluated. Interestingly, the methylation levels of CSC (+) tumors were significantly higher than the levels in CSC (–) tumors ($p = 0.009$). Although CSC (+) cases had higher methylation levels, their median survival time was shorter. In the current study, *MGMT* methylation level of cases was only evaluated with EpiTect Methyl II PCR Assays. Although analyze was confirmed with MSP, a further validation with bisulfite Sanger sequencing may increase the accuracy of our data about *MGMT* methylation rates. Additionally, the

number of CSC (+) cases were limited in this study, thus, to obtain more reliable data, promoter methylation status of CSC (+) cases may be evaluate in a larger group. For all that, in a study by Melguizo et al., the correlation between the CD133 status and *MGMT* protein expression levels was analyzed in GBM tumors; no correlation was reported (Melguizo et al. 2012). In addition, there are a number of studies reporting that GBM patients with unmethylated tumors experience unexpected favorable outcomes after receiving radiochemotherapy, and some patients with a methylated promoter do not benefit from concomitant and adjuvant TMZ treatment (Everhard et al. 2009; Ramakrishnan et al. 2011). Therefore, *MGMT* methylation may not be the only mechanism responsible for chemotherapy resistance in GBM (Kreth et al. 2013). According to Kreth et al., after transfection of miR-181d, miR-767-3p, and miR-648 to T98G cell lines, responsivity of cells to TMZ was significantly enhanced. In addition, Kreth et al. suggest that miR-181d, miR-767-3p, and miR-648 as significant post-transcriptional regulators of *MGMT* and miR-181d and miR-767-3p may induce *MGMT* mRNA degradation, the latter affects *MGMT* protein translation. Thus,

Fig. 3 Bcl2 and Smad2 expression by immunohistochemistry ($\times 100$). **a** Bcl2 expression $>10\%$, **b** Bcl2 expression $<10\%$, **c** Smad2 cytoplasmic and nuclear positive staining, **d** Smad2 nuclear positive staining

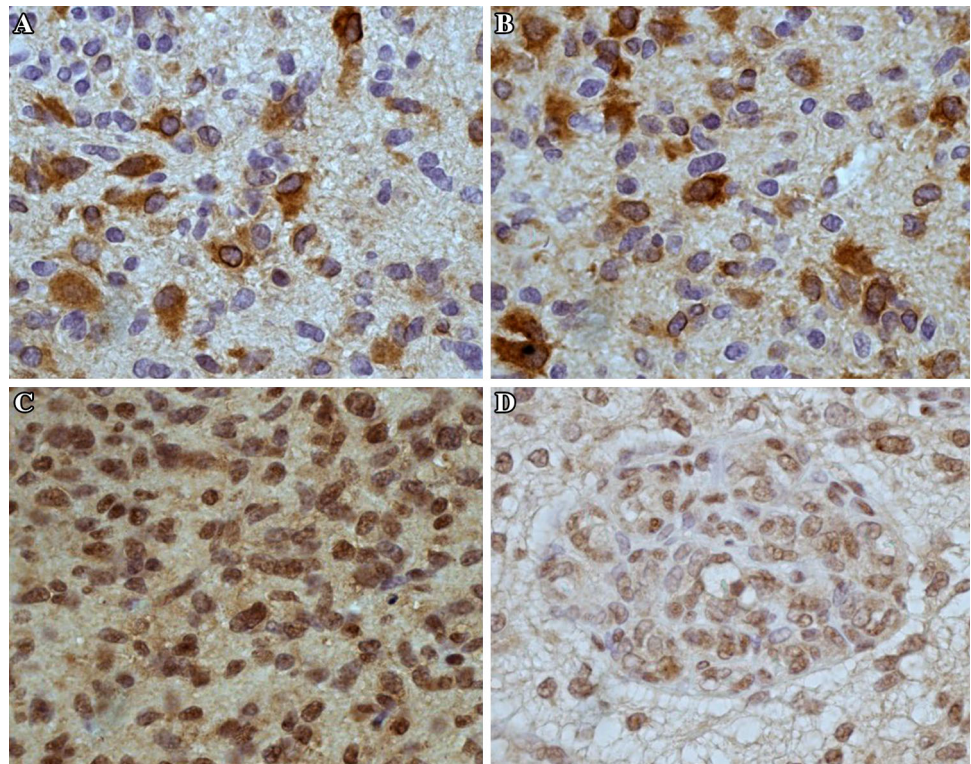


Table 6 Correlations between miRNA expressions and Bcl2 and Smad2 protein levels

miRNA	Correlation (r value) with Bcl2 staining	p value
miR-181b	-0.265	0.258
miR-153	-0.394	0.085
miR-137	-0.372	0.106
miR-145	-0.218	0.355
miR-10a	-0.193	0.416
miR-10b	-0.219	0.354
Let-7d	-0.214	0.365
miR-9	-0.151	0.524
	Correlation (r value) with cytoplasmic Smad2 staining	
miR-455-3p	-0.653	0.002
	Correlation (r value) with nuclear Smad2 staining	
miR-455-3p	-0.174	0.463

elongation of the 3'-UTR of *MGMT* gene mRNA may cause an alternatively polyadenylated transcript that is susceptible to miRNA-mediated suppression instead of promoter methylation and response to chemotherapy may also be modulated by miRNA expression (Kreth et al. 2013). In the current study, we compared the expression levels of nine miRNAs with functions related to chemoresistance in CSC (+) and CSC (-) GBM tumors (Zhu et al. 2010; Ujifuku et al. 2010; Takwi et al. 2013; Zhu

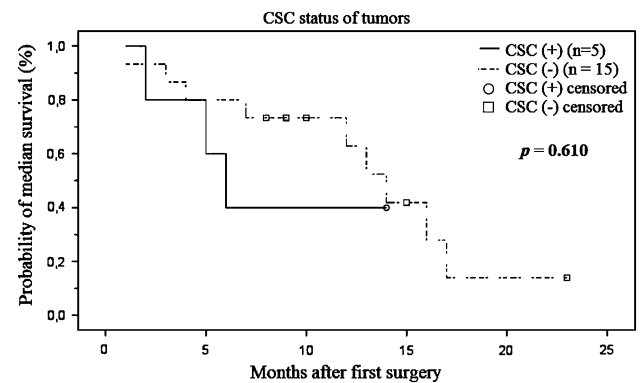


Fig. 4 Kaplan–Meier plots of the median survival probability of GBM patients with CSCs versus without CSCs

et al. 2013; Munoz et al. 2013; Jeon et al. 2011; Nishida et al. 2012; Zhang et al. 2013; Shi et al. 2012; Wang et al. 2013; Hummel et al. 2010; Li et al. 2009; M-Chang et al. 2011). We found that miR-455-3p is upregulated, and miR-181b, miR-153, miR-137, miR-145, let-7d, and miR-9 are downregulated in CSC (+) cases. Because this study was limited to 9 miRNAs that were previously described in GBM research, we could not identify unknown miRNAs involved in CSC progression in our study cohort. According to our findings, miR-181b was downregulated more than 100-fold (0.0055) ($p = 0.053$), and miR-455-3p was upregulated more than 53.64-fold ($p = 0.004$) in CSC

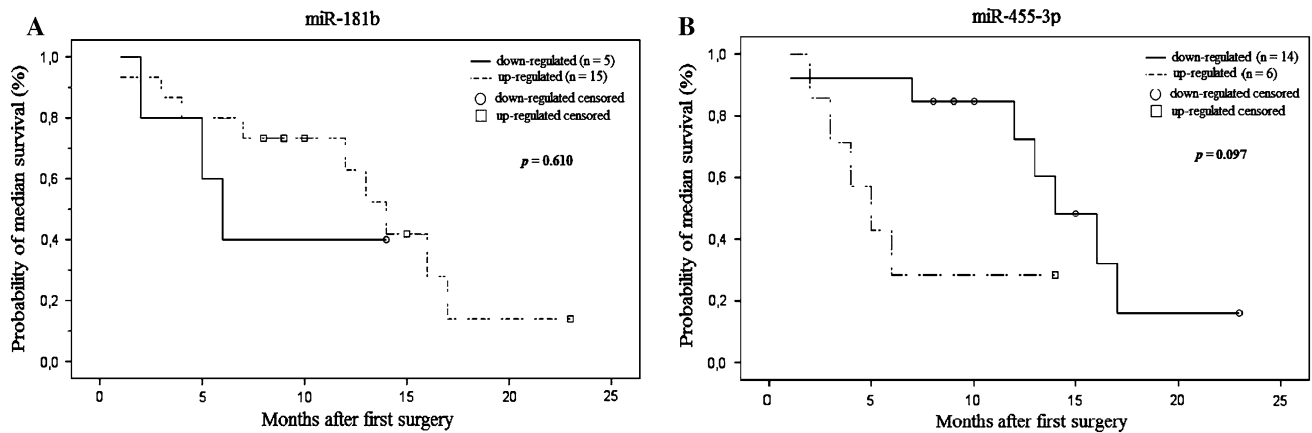


Fig. 5 Kaplan–Meier plots of the median survival probability of GBM patients with upregulated versus downregulated expression of **a** miR-181b and **b** miR-455-3p

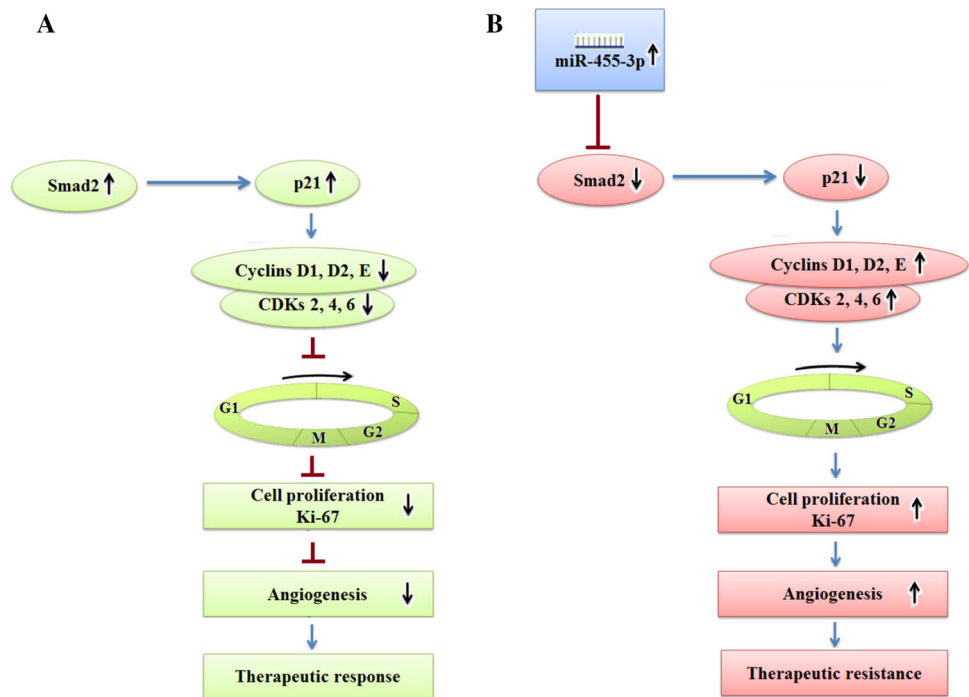
(+) tumors when compared to CSC (–) tumors. Therefore, we suggest that altered expression of miR-181b and miR-455-3p may cause TMZ resistance in CSC (+) GBM tumors.

To date, the CSC miR-10b, miR-153, and miR-137 expression levels in GBM have been targeted for study (Guessous et al. 2013; Zhao et al. 2013; Bier et al. 2013). In the current study, our results showed lower expression levels of miR-10b (1.95-fold), miR-153 (3.03-fold), and miR-137 (2.53-fold) in CSC (+) tumors when compared to CSC (–) tumors, but the differences were not significant ($p > 0.05$). Because of the difficulties associated with studying primary tumors, the miRNAs were analyzed using a small study cohort. We evaluated miRNAs in 5 CSC (+) and 15 CSC (–) cases, from a total of 20 primary GBM specimens. We suggest that this limited sample size may have prevented us from identifying several miRNAs with potentially significant roles in CSC progression in our patient population. Studies with higher sample sizes may reveal more accurate data for these miRNAs. In previous studies, the upregulations of miR-10a and miR-9 were also linked to TMZ resistance in GBM cell lines (Ujifuku et al. 2010; Munoz et al. 2013). In our study, the expression of these miRNAs in primary GBM tumors depended on the presence of CSCs. Although CSC (+) cases are chemoresistant, miR-10a expression was 1.71-fold and miR-9 expression more than 100-fold (0.0059) lower than in CSC (–) cases ($p = 0.114$, $p = 0.266$, respectively). Reduced expression of the let-7 miRNA families is associated with low responsiveness to a number of chemotherapeutic agents (Hummel et al. 2010). Lee et al. showed that transfection of let-7 miRNA suppressed the expression of *pan-RAS*, *N-RAS*, and *K-RAS* in GBM cells and also decreased in vitro proliferation and migration of cells as well as the tumor size after transplantation into nude mice (Lee et al. 2011). Although reduced expression level of let-

7d has determined in GBM tumors previously, strongly decreased expression of let-7d (more than 100 fold; 0.0024) first identified in CSC (+) GBM tumors in the current study ($p = 0.109$). The function of miR-145 in GBM tumors is a controversial topic. In 2012, Koo et al. first reported over-expression of miR-145 in GBM cell lines and asserted that miR-145 was associated with invasion (Koo et al. 2012). In contrast, one of our previous studies reported decreased miR-145 expression in the T98G GBM cell line (Tunca et al. 2012). Several other studies confirm our findings, reporting decreased expression of miR-145 in GBM tumors (Rani et al. 2013; Lee et al. 2013; Haapa-Paananen et al. 2013). Rani et al. reported the reduced regulation of miR-145 in a graded manner, with GBM patients showing the lowest expression levels relative to low-grade gliomas (Rani et al. 2013). Similarly, in a recent study, Lee et al. compared the expression levels of miR-145 between glioma cells and normal astrocytes and between CSCs and neural stem cells; miR-145 was significantly downregulated in glioma cells and CSCs compared to normal astrocytes and neural stem cells. Low expression of miR-145 was also linked to poor patient prognosis. In addition, transfection of miR-145 to glioma cells significantly decreased migration and invasion (Lee et al. 2013). In the present study, miR-145 expression was 32-fold lower in CSC (+) tumors than in CSC (–) tumors ($p = 0.120$). This is the first data in the literature reporting different miR-145 expression levels in CSC (+) and CSC (–) tumors.

Reduced expression of miR-181b in brain tumors has been reported in previous studies (Haapa-Paananen et al. 2013). However, there is only one study evaluating miR-181b expression in gliomas that distinguishes between expression in CSC (+) and CSC (–) tumors. In that study, miR-181b was analyzed for its biological effect on CSCs derived from U-87 cells using FACS sorting. That study is

Fig. 6 A schematic summarizing the hypothesis of miR-455-3p's effects in TGF- β -Smad signaling pathway. **a** In non-tumoral tissues and low-grade tumors, phosphorylation of Smad2 leads to cell proliferation. **b** In CSC (+) cells, silencing of Smad2 by miR-455-3p induces of cell proliferation



consistent with our results, reporting that miR-181b was downregulated in CSCs and that upregulation of this miRNA suppressed proliferation and reduced chemoresistance to TMZ (Li et al. 2010). In the present study, Kaplan–Meier plots also revealed that patients with reduced miR-181b expression had shorter median survival times. Although we determined significant differences in both the miR-181b expression levels and *MGMT* methylation rates between CSC (+) and CSC (–) tumors, there was no correlation between the miR-181b expression and *MGMT* methylation. Wang et al. (2013) also analyzed the association of the miR-181b expression and *MGMT* methylation in glioma cells and did not report any correlation. They demonstrated that miR-181b bound directly to the 3' untranslated regions of *MEK1* and enhanced TMZ sensitivity via *MEK1* downregulation (Wang et al. 2013). *MEK1*, also known as MAP2K1, is involved in the mitogen-activated protein kinase (MAPK) pathway which is highly activated in high-grade gliomas and plays role in regulation of chemosensitivity (Wu et al. 2005; Valledor et al. 2008; Hirata et al. 2012; Jones et al. 2008). Also, it was demonstrated in a study of CSC (+) GBM tumors that inhibition of MEK reduced MDM2 expression and caused downregulation of *MGMT* expression via activation of p53 (Sato et al. 2011). Thus, miR-181b and *MEK1* interaction may lead to inhibition *MGMT* via MAPK-ERK pathway. According to the miRWalk database and recent studies, the predicted target genes of miR-181b are *ATM*, *BCL2*, *TGF- β* , *TIMP3*, and *MCL-1* (Bisso et al. 2013; Zhu et al. 2010, 2012; Calin et al. 2007; Wang et al. 2012, 2010; Visone

et al. 2011). In the current study, we analyzed the protein expression levels of Bcl2 in FFPE GBM sections taken from CSC (+) and (–) cases. In previous studies, the ability of miR-181b to modulate multidrug resistance by targeting *BCL2* was demonstrated in gastric and lung cancer cell lines (Zhu et al. 2010), and transfection of miR-181b reportedly increased cell apoptosis in GBM (Shi et al. 2008). However, in the current study, no significant correlation was found between the miR-181b and Bcl2 expression levels. We suggest that because Bcl2 is regulated by different miRNAs, the relationship between miR-181b and Bcl2 could be more accurately evaluated with a larger the study. On the other hand, the results of the current study may suggest that miR-181b levels may be a marker for determining TMZ sensitivity in *MGMT* methylated and CSC (+) GBM patients.

There seems to be only one published paper focusing on the role that miR-455-3p plays in TMZ resistance in GBM cells (Ujifuku et al. 2010). Ujifuku et al. analyzed the role of miR-455-3p in the GBM cell lines U251 Wt and U251 R, which are fully methylated to avoid the effect of *MGMT* methylation on the TMZ response. The authors of that study suggest that suppression of miR-455-3p may have a cell-killing effect in the presence of TMZ (Ujifuku et al. 2010). In the current study, we uniquely demonstrated that miR-455-3p is 53.6-fold upregulated in CSC (+) GBM tumors that are TMZ resistant even though they contain methylated *MGMT* genes. In addition, according to Kaplan–Meier analyses, patients with higher miR-455-3p expression had shorter median survival times. Therefore,

we suggest that high levels of miR-455-3p expression may potentially cause TMZ resistance via a *MGMT*-independent pathway in CSC (+) GBM tumors. After consulting the miRWalk database and recent studies, we identified *SMAD2*, *ACVR2B*, *LTBR*, and *EI24* as predicted targets for miR-455-3p (Swingler et al. 2012; Ujifuku et al. 2010). Because the TGF- β -Smad pathway has a crucial role in drug resistance in GBM (Sze et al. 2013), in the current study, Smad2 stainings of FFPE tumor sections of CSC (+) and CSC (–) cases were analyzed. CSC (+) cases showed lower Smad2 protein expression levels than CSC (–) cases when analyzing both nuclear and cytoplasmic immunohistochemical stainings. According to Bruna A et al., although TGF- β acts as a tumor suppressor in early-stage tumors, it becomes an oncogenic factor in advanced tumors. Therefore, aggressive and highly proliferative gliomas may demonstrate high TGF- β -Smad activity (Bruna et al. 2007). In addition, previous studies suggest that the expression of miR-455 may be induced by TGF and *Activin* (Swingler et al. 2012). On the other hand, according to Zhang L et al., *SMAD2* expression is lower in glioma cells than in normal astrocytes (Zhang et al. 2006). We hypothesize that *SMAD2* may be suppressed via high miR-455-3p expression in CSC (+) cases (Fig. 6). Pearson correlation analysis revealed a significant negative correlation between miR-455-3p and cytoplasmic Smad2 expression levels in tumors ($p = 0.002$). According to immunohistochemical analyses, Smad2 expression was not only reduced in cytoplasm but also in nucleus of the CSC (+) cases. Therefore, we suppose high miR-455-3p expression might be inhibiting Smad2 expression in cytoplasm, preventing the Smad2/3 complex from transporting into the nucleus. Similar to this hypothesis, Swingler et al. (2012) suggested that miR-455-3p had a silencing effect on Smad2 in the cytoplasm of osteoarthritis cells. We suggest that one of the causes of the resistance to a TGF- β -mediated growth inhibition in CSC (+) GBM tumors might be the result of increased miR-455-3p expression. Thus, the regulation of miR-455-3p might be a useful prognostic biomarker for TMZ resistance in CSC (+) GBM cases.

In conclusion, we demonstrated that low miR-181b and high miR-455-3p expression levels might be significant prognostic factors for TMZ resistance in *MGMT* methylated CSC (+) GBM patients ($p = 0.053$, $p = 0.004$; respectively). Thus, these observations suggest that modulation of miRNA expression may be another important mechanism underlying the chemoresistance of GBM. To the best of our knowledge, this is the first time that the altered miR-455-3p expression has been correlated with TMZ resistance in CSC (+) primary GBM tumors. Therefore, advanced studies of the silencing of miR-455-3p in GBM may help *MGMT* methylated GBM patients overcome TMZ resistance. In addition, understanding the

precise role of miR-455-3p in GBM progression, depending on the CSC status, will increase our understanding of GBM biology and may provide novel therapeutic molecular targets for treating GBM.

Acknowledgments This study was supported by a grant from the Scientific Research Projects Foundation (BAP) of the Uludag University of Turkey [Project No. OUAP (T)-2012/17].

Conflict of interest None.

References

- Altaner C (2008) Glioblastoma and stem cells. *Neoplasma* 55:369–374
- Bartel DP (2009) MicroRNAs: target recognition and regulatory functions. *Cell* 136:215–233
- Bier A, Giladi N, Kronfeld N et al (2013) MicroRNA-137 is downregulated in glioblastoma and inhibits the stemness of glioma stem cells by targeting RTVP-1. *Oncotarget* 4(5):665–676
- Bisso A, Faleschini M, Zampa F et al (2013) Oncogenic miR-181a/b affect the DNA damage response in aggressive breast cancer. *Cell Cycle* 12(11):1679–1687
- Brescia P, Ortensi B, Fornasari L et al (2013) CD133 is essential for glioblastoma stem cell maintenance. *Stem Cells* 31(5):857–869
- Bruna A, Darken RS, Rojo F et al (2007) High TGFbeta-Smad activity confers poor prognosis in glioma patients and promotes cell proliferation depending on the methylation of the PDGF-B gene. *Cancer Cell* 11(2):147–160
- Calin GA, Croce CM (2006) MicroRNA signatures in human cancers. *Nat Rev Cancer* 6:857–866
- Calin GA, Pekarsky Y, Croce CM (2007) The role of microRNA and other non-coding RNA in the pathogenesis of chronic lymphocytic leukemia. *Best Pract Res Clin Haematol* 20(3):425–437
- Cecener G, Tunca B, Egeli U et al (2012) The promoter hypermethylation status of GATA6, MGMT, and FHIT in glioblastoma. *Cell Mol Neurobiol* 32(2):237–244
- Cheng WY, Kandel JJ, Yamashiro DJ et al (2012) A multi-cancer mesenchymal transition gene expression signature is associated with prolonged time to recurrence in glioblastoma. *PLoS One* 7(4):e34705
- Dirks PB (2005) Brain tumor stem cells. *Biol Blood Marrow Transpl* 11(2 Suppl 2):12–13
- Esquela-Kerscher A, Slack FJ (2006) Oncomirs-microRNAs with a role in cancer. *Nat Rev Cancer* 6:259–269
- Everhard S, Tost J, El Abdalaoui H et al (2009) Identification of regions correlating MGMT promoter methylation and gene expression in glioblastomas. *Neuro Oncol* 11(4):348–356
- Galli R, Binda E, Orfanelli U (2004) Isolation and characterization of tumorigenic, stem-like neural precursors from human glioblastoma. *Cancer Res* 64:7011–7021
- Guessous F, Alvarado-Velez M, Marcinkiewicz L et al (2013) Oncogenic effects of miR-10b in glioblastoma stem cells. *J Neurooncol* 112(2):153–163
- Haapa-Paananen S, Chen P, Hellström K et al (2013) Functional profiling of precursor MicroRNAs identifies MicroRNAs essential for glioma proliferation. *PLoS One* 8(4):e60930
- Hegi ME, Diserens AC, Gorlia T et al (2005) MGMT gene silencing and benefit from temozolomide in glioblastoma. *N Engl J Med* 352(10):997–1003
- Hemmati HD, Nakano I, Lazareff JA et al (2003) Cancerous stem cells can arise from pediatric brain tumors. *Proc Natl Acad Sci USA* 100:15178–15183

- Hirata H, Hinoda Y, Ueno K et al (2012) MicroRNA-1826 targets VEGFC, beta-catenin (CTNNB1) and MEK1 (MAP2K1) in human bladder cancer. *Carcinogenesis* 33(1):41–48
- Hummel R, Hussey DJ, Haier J (2010) MicroRNAs: predictors and modifiers of chemo- and radiotherapy in different tumour types. *Eur J Cancer* 46(2):298–311
- Ichimura K, Pearson DM, Kocalkowski S et al (2009) IDH1 mutations are present in the majority of common adult gliomas but rare in primary glioblastomas. *Neuro Oncol* 11(4):341–347
- Ignatova TN, Kukekov VG, Laywell ED et al (2002) Human cortical glial tumors contain neural stem-like cells expressing astroglial and neuronal markers in vitro. *Glia* 39:193–206
- Jeon HM, Sohn YW, Oh SY et al (2011) ID4 imparts chemoresistance and cancer stemness to glioma cells by derepressing miR-9*-mediated suppression of SOX2. *Cancer Res* 71(9):3410–3421
- Jones DT, Kocalkowski S, Liu LETAL (2008) Tandem duplication producing a novel oncogenic BRAF fusion gene defines the majority of pilocytic astrocytomas. *Cancer Res* 68(21):8673–8677
- Kloth JN, Kenter GG, Spijker HS et al (2008) Expression of Smad2 and Smad4 in cervical cancer: absent nuclear Smad4 expression correlates with poor survival. *Mod Pathol* 21(7):866–875
- Koo S, Martin GS, Schulz KJ et al (2012) Serial selection for invasiveness increases expression of miR-143/miR-145 in glioblastoma cell lines. *BMC Cancer* 10(12):143
- Kreth S, Limbeck E, Hinske LC et al (2013) In human glioblastomas transcript elongation by alternative polyadenylation and miRNA targeting is a potent mechanism of MGMT silencing. *Acta Neuropathol* 125(5):671–681
- Lathia JD, Gallagher J, Myers JT et al (2011) Direct in vivo evidence for tumor propagation by glioblastoma cancer stem cells. *PLoS One* 6(9):e24807
- Lee ST, Chu K, Oh HJ et al (2011) Let-7 microRNA inhibits the proliferation of human glioblastoma cells. *J Neurooncol* 102:19–24
- Lee HK, Bier A, Cazacu S et al (2013) MicroRNA-145 is downregulated in glial tumors and regulates glioma cell migration by targeting connective tissue growth factor. *PLoS One* 8(2):e54652
- Leibetseder A, Ackerl M, Flechl B et al (2013) Outcome and molecular characteristics of adolescent and young adult patients with newly diagnosed primary glioblastoma: a study of the Society of Austrian Neurooncology (SANO). *Neuro Oncol* 15(1):112–121
- Lewis BP, Burge CB, Bartel DP (2005) Conserved seed pairing, often flanked by adenosines, indicated that thousands of human genes are microRNA targets. *Cell* 120:15–20
- Li Y, VandenBoom TG 2nd, Kong D et al (2009) Up-regulation of miR-200 and let-7 by natural agents leads to the reversal of epithelial-to-mesenchymal transition in gemcitabine-resistant pancreatic cancer cells. *Cancer Res* 69(16):6704–6712
- Li P, Lu X, Wang Y et al (2010) MiR-181b suppresses proliferation and reduces chemoresistance to temozolomide in U87 glioma stem cells. *J Biomed Res* 24(6):436–443
- Liu G, Yuan X, Zeng Z et al (2006) Analysis of gene expression and chemoresistance of CD133+ cancer stem cells in glioblastoma. *Mol Cancer* 5:67
- Livak KJ, Schmittgen TD (2001) Analysis of relative gene expression data using real-time quantitative PCR and the $2^{-\Delta\Delta C(T)}$ method. *Methods* 25:402–408
- Louis DN, Ohgaki H, Wiestler OD et al (2007) The 2007 WHO classification of tumours of the central nervous system. *Acta Neuropathol* 114:97–109
- M-Chang CJ, Hsu CC, Chang CH et al (2011) Let-7d functions as novel regulator of epithelial-mesenchymal transition and chemoresistant property in oral cancer. *Oncol Rep* 26(4):1003–1010
- Melguizo C, Prados J, González B et al (2012) MGMT promoter methylation status and MGMT and CD133 immunohistochemical expression as prognostic markers in glioblastoma patients treated with temozolomide plus radiotherapy. *J Transl Med* 17(10):250
- Munoz JL, Bliss SA, Greco SJ et al (2013) Delivery of functional anti-miR-9 by mesenchymal stem cell-derived exosomes to glioblastoma multiforme cells conferred chemosensitivity. *Mol Ther Nucleic Acids* 1(2):e126
- Nakano I, Kornblum HI (2006) Brain tumor stem cells. *Pediatr Res* 59(4 Pt 2):54R–58R
- Nishida N, Yamashita S, Mimori K et al (2012) MicroRNA-10b is a prognostic indicator in colorectal cancer and confers resistance to the chemotherapeutic agent 5-fluorouracil in colorectal cancer cells. *Ann Surg Oncol* 19(9):3065–3071
- Nobusawa S, Watanabe T, Kleihues P et al (2009) IDH1 mutations as molecular signature and predictive factor of secondary glioblastomas. *Clin Cancer Res* 15(19):6002–6007
- Okamoto OK, Oba-Shinjo SM, Lopes L et al (2007) Expression of HOXC9 and E2F2 are up-regulated in CD 133+ cells isolated from human astrocytomas and associated with transformation of human astrocytes. *Biochim Biophys Acta* 1769:437–442
- Oliver TG, Wechsler-Reya RJ (2004) Getting at the root and stem of brain tumors. *Neuron* 42:885–888
- Persano L, Pistollato F, Rampazzo E et al (2012) BMP2 sensitizes glioblastoma stem-like cells to Temozolomide by affecting HIF-1 α stability and MGMT expression. *Cell Death Dis* 18(3):e412
- Pistollato F, Abbadì S, Rampazzo E et al (2010) Intratumoral hypoxic gradient drives stem cells distribution and MGMT expression in glioblastoma. *Stem Cells* 28:851–862
- Ramakrishnan V, Kushwaha D, Koay DC et al (2011) Post-transcriptional regulation of O(6)-methylguanine-DNA methyltransferase MGMT in glioblastomas. *Cancer Biomark* 10(3–4):185–193
- Rani SB, Rathod SS, Karthik S et al (2013) MiR-145 functions as a tumor-suppressive RNA by targeting Sox9 and adducin 3 in human glioma cells. *Neuro Oncol* 15(10):1302–1316
- Revelos K, Petraki C, Gregorakis A et al (2005) Immunohistochemical expression of Bcl2 is an independent predictor of time-to-biochemical failure in patients with clinically localized prostate cancer following radical prostatectomy. *Anticancer Res* 25(4):3123–3133
- Reya T, Morrison SJ, Clarke MF et al (2001) Stem cells, cancer, and cancer stem cells. *Nature* 414:105–111
- Rorke LB (1997) Pathologic diagnosis as the gold standard. *Cancer* 79:665–667
- Sanchez-Martin M (2008) Brain tumour stem cells: implications for cancer therapy and regenerative medicine. *Curr Stem Cell Res Ther* 3:197–207
- Sato A, Sunayama J, Matsuda K et al (2011) MEK-ERK signaling dictates DNA-repair gene MGMT expression and temozolomide resistance of stem-like glioblastoma cells via the MDM2-p53 axis. *Stem Cells* 29(12):1942–1951
- Shi L, Cheng Z, Zhang J et al (2008) hsa-mir-181a and hsa-mir-181b function as tumor suppressors in human glioma cells. *Brain Res* 1236:185–193
- Shi M, Du L, Liu D et al (2012) Glucocorticoid regulation of a novel HPV-E6-p53-miR-145 pathway modulates invasion and therapy resistance of cervical cancer cells. *J Pathol* 228(2):148–157
- Singh SK, Clarke ID, Terasaki M et al (2003) Identification of a cancer stem cell in human brain tumors. *Cancer Res* 63:5821–5828
- Stupp R, Hegi ME, Mason WP et al (2009) Effects of radiotherapy with concomitant and adjuvant temozolomide versus radiotherapy alone on survival in glioblastoma in a randomised phase III study: 5-year analysis of the EORTC-NCIC trial. *Lancet Oncol* 10(5):459–466
- Swingler TE, Wheeler G, Carmont V et al (2012) The expression and function of microRNAs in chondrogenesis and osteoarthritis. *Arthritis Rheum* 64(6):1909–1919

- Sze CI, Su WP, Chiang MF et al (2013) Assessing current therapeutic approaches to decode potential resistance mechanisms in glioblastomas. *Front Oncol* 19(3):59
- Takwi AA, Wang YM, Wu J et al (2013) miR-137 regulates the constitutive androstane receptor and modulates doxorubicin sensitivity in parental and doxorubicin-resistant neuroblastoma cells. *Oncogene*. doi:10.1038/onc.2013.330
- Tunca B, Tezcan G, Cecener G et al (2012) *Olea europaea* leaf extract alters microRNA expression in human glioblastoma cells. *J Cancer Res Clin Oncol* 138(11):1831–1844
- Ujifuku K, Mitsutake N, Takakura S et al (2010) miR-195, miR-455-3p and miR-10a(*) are implicated in acquired temozolomide resistance in glioblastoma multiforme cells. *Cancer Lett* 296(2):241–248
- Valledor AF, Arpa L, Sanchez-Tillo E et al (2008) IFN- γ -mediated inhibition of MAPK phosphatase expression results in prolonged MAPK activity in response to M-CSF and inhibition of proliferation. *Blood* 112(8):3274–3282
- Visone R, Veronese A, Rassenti LZ et al (2011) miR-181b is a biomarker of disease progression in chronic lymphocytic leukemia. *Blood* 118(11):3072–3079
- Wang B, Hsu SH, Majumder S et al (2010) TGF β -mediated upregulation of hepatic miR-181b promotes hepatocarcinogenesis by targeting TIMP3. *Oncogene* 29(12):1787–1797
- Wang B, Li W, Guo K et al (2012) miR-181b promotes hepatic stellate cells proliferation by targeting p27 and is elevated in the serum of cirrhosis patients. *Biochem Biophys Res Commun* 421(1):4–8
- Wang J, Sai K, Chen FR et al (2013) miR-181b modulates glioma cell sensitivity to temozolomide by targeting MEK1. *Cancer Chemother Pharmacol* 72(1):147–158
- Weller M, Pfister SM, Wick W et al (2013) Molecular neuro-oncology in clinical practice: a new horizon. *Lancet Oncol* 14(9):e370–e379
- Wu W, Pew T, Zou M et al (2005) Glucocorticoid receptor-induced MAPK phosphatase-1 (MPK-1) expression inhibits paclitaxel-associated MAPK activation and contributes to breast cancer cell survival. *J Biol Chem* 280(6):4117–4124
- Zhang L, Sato E, Amagasaki K et al (2006) Participation of an abnormality in the transforming growth factor- β signaling pathway in resistance of malignant glioma cells to growth inhibition induced by that factor. *J Neurosurg* 105:119–128
- Zhang L, Pickard K, Jenei V et al (2013) miR-153 supports colorectal cancer progression via pleiotropic effects that enhance invasion and chemotherapeutic resistance. *Cancer Res* 73(21):6435–6447
- Zhao S, Deng Y, Liu Y et al (2013) MicroRNA-153 is tumor suppressive in glioblastoma stem cells. *Mol Biol Rep* 40(4):2789–2798
- Zhu W, Shan X, Wang T et al (2010) miR-181b modulates multidrug resistance by targeting BCL2 in human cancer cell lines. *Int J Cancer* 127(11):2520–2529
- Zhu DX, Zhu W, Fang C et al (2012) miR-181a/b significantly enhances drug sensitivity in chronic lymphocytic leukemia cells via targeting multiple anti-apoptosis genes. *Carcinogenesis* 33(7):1294–1301
- Zhu X, Li Y, Shen H et al (2013) miR-137 restoration sensitizes multidrug-resistant MCF-7/ADM cells to anticancer agents by targeting YB-1. *Acta Biochim Biophys Sin (Shanghai)* 45(2):80–86